# Poincaré wave-induced shear instability in Lake Michigan

TC Hsieh[1](tchsieh@purdue.edu ), Cary Troy[1], and Nathan Hawley[2]
1. School of Civil Engineering, Purdue University, West Lafayette, IN, 47906
2. NOAA Great Lakes Environmental Research Laboratory, 4840 S. State road., Ann Arbor, Michigan 48108

## Introduction

Cross-thermocline mixing is an important process during the stratified period in the Great Lakes, especially in the lake interiors. Recent evidence suggests that the basin-scale mixing in world's largest lakes may actually occur primarily in the lake interiors. Several years of velocity and temperature data are examined from the south basin of Lake Michigan in order to examine the processes that are potentially responsible for cross-thermocline mixing. Near-inertial internal Poincaré waves are shown to thoroughly dominate the thermocline currents and in turn provide most of the observed thermocline shear in Lake Michigan's deeper waters. Calculated Richardson numbers and stability analysis both suggest that these waves do cause cross-thermocline mixing, and hence high resolution measurements are necessary to better quantify turbulent mixing in the interior of Lake Michigan.
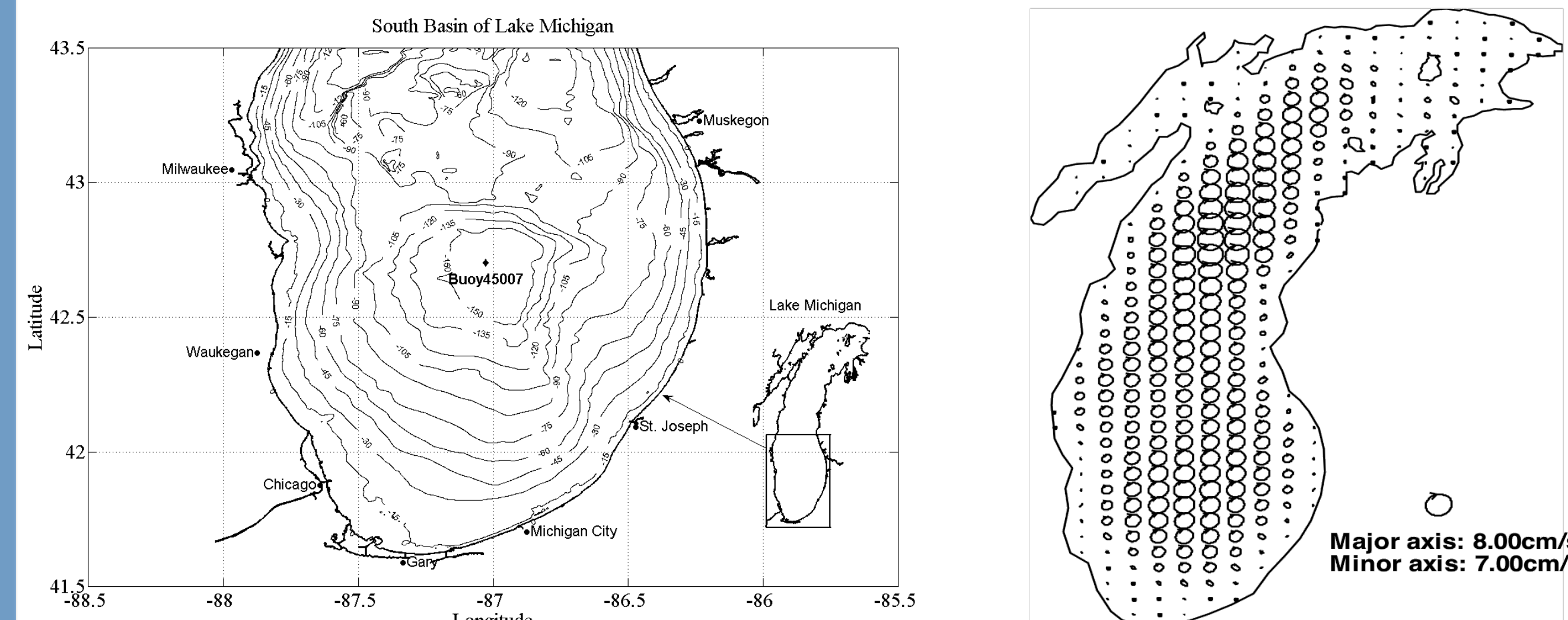
## Structure of Internal Poincaré Waves



**Fig. 1. Measurement location.** Two acoustic Doppler velocimeters and one thermister chain were deployed at the location where Buoy 45007 was. It is also at the center of the south basin of Lake Michigan. We chose this location because of its simpler bathymetry and the deep water depth, about 150m. The wave motion in this region can thus be regarded as free from any bottom boundary or shoreline effects.

**Fig. 2. Spatial structure of internal Poincaré waves.** Current ellipses of the internal Poincaré waves from SUNTANS numerical simulation. The total combined response to the wind forcing appears to show east-west mode 1 structure for thermocline displacements, and a two-celled structure for near-surface velocities. Large velocities are seen in locations of deepest water, i.e. the centers of the northern and southern basins. (Source: Sultan Ahmed per com.)
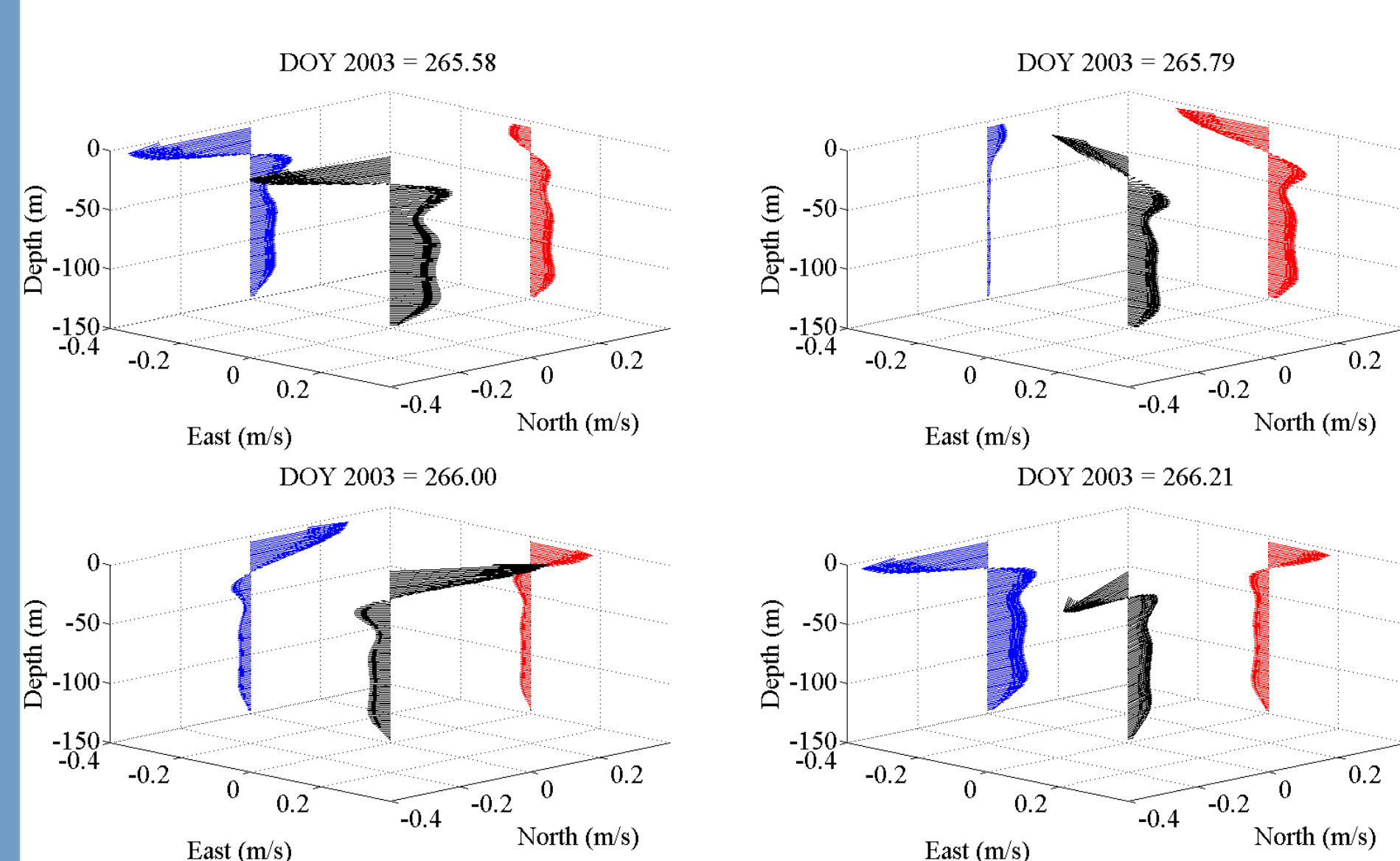
**Fig. 3. Rotating structure of internal Poincaré waves.** This figure shows the axisymmetric clockwise rotating structure of the internal Poincaré waves from the ADCP measurements during the stratification season. The **black** profile indicates the resultant velocity of the measured two components. The **red** is its projection onto the **east-west** plane; while the **blue** is that onto the **north-south** plane. The most elevated shear appears in the depth above 60m where the thermocline presents. This constitutes two major assumptions. First, the internal Poincaré waves are responsible for the elevated shear in the interior of the water column during the stratification season. Second, the velocity profile is axisymmetric.

**Fig. 4. Normal-mode-calculated velocity vs. measured one.** (a) is the background temperature profile, and (b) and (c) are the velocity profiles from ADCP (solid) and normal-mode calculations (dashed). Because of the axisymmetric feature of the resultant velocity profile, we attempted to use the calculated normal-mode velocity to approximate the measured velocity for the later use of the stability analysis. Although, the measured velocity profiles compose not only just one mode of the wave modes, the calculated normal-mode solution can still capture a relatively comparable shape of the velocity profile.
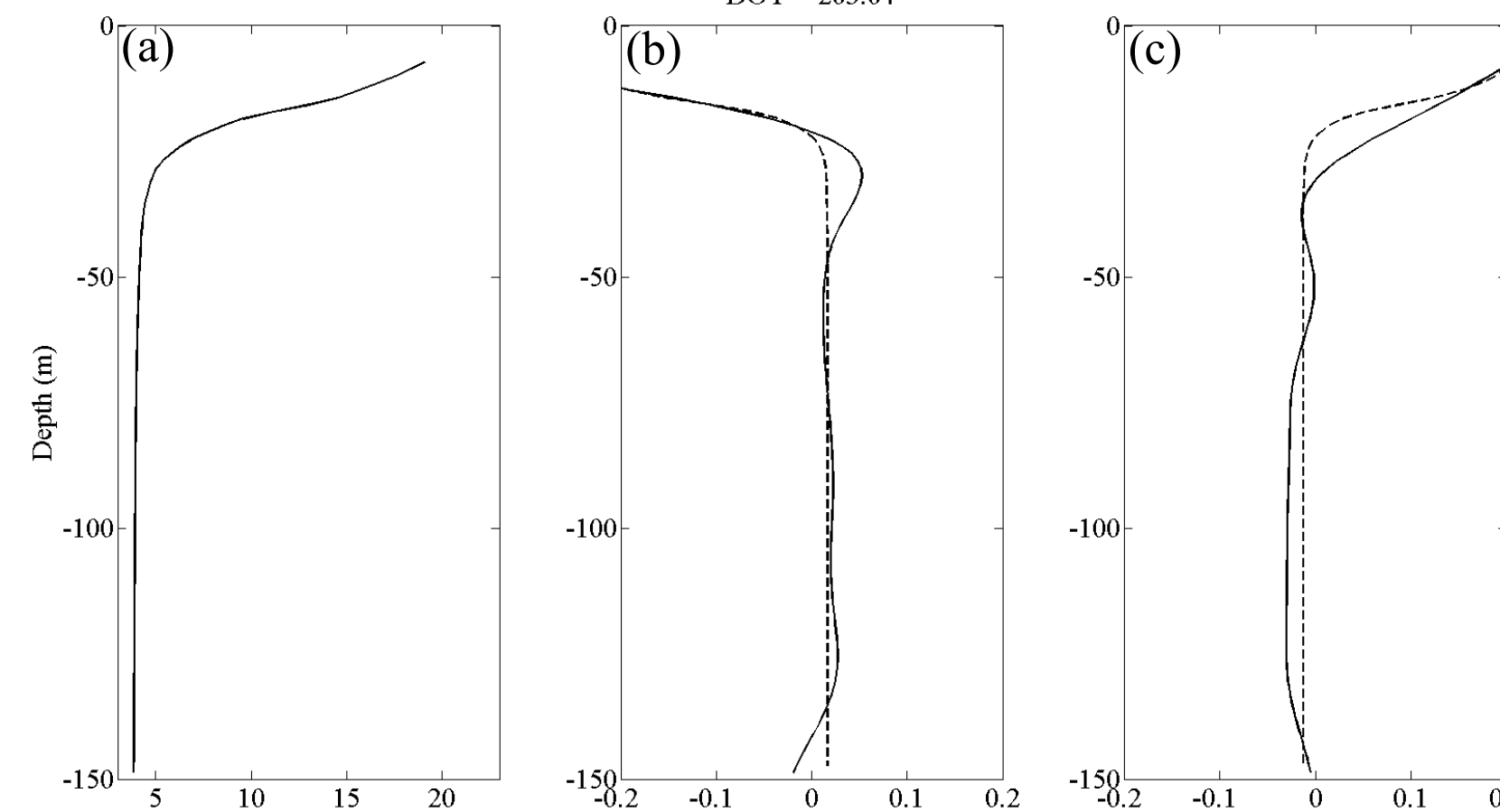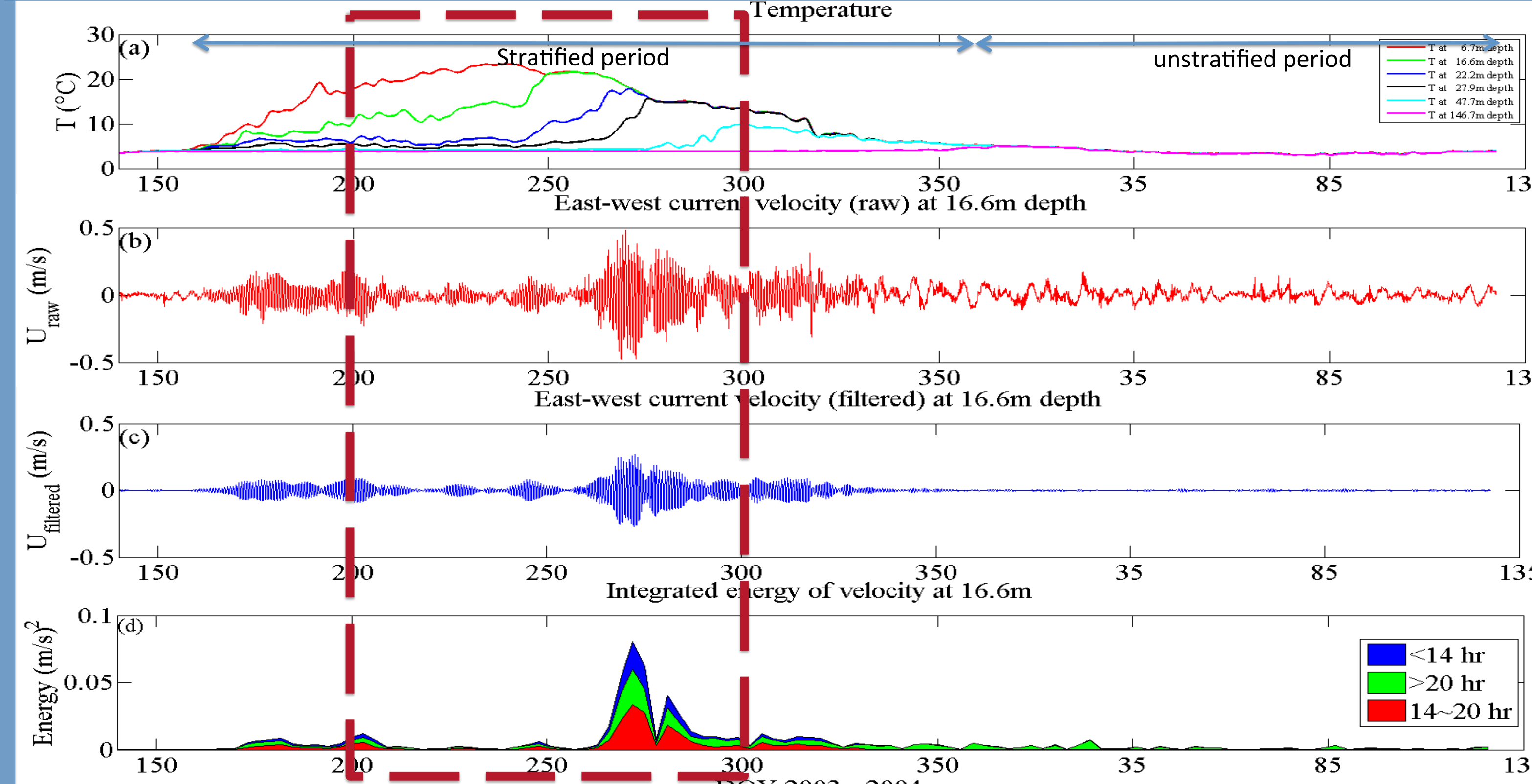
## Seasonal Variations



**Fig. 5. Seasonal variations of temperature, velocity, and energy.** This figure shows the year-long variation of (a) temperature at 6.7, 16.6, 22.2, 27.9, 47.7, and 146.7m depths; (b) the raw east-west current velocity at the depth of 16.6m; (c) the same setup for the low-pass filtered current; (d) integrated energy of the near-inertial period (~14-20hr), the super-inertial and sub-inertial periods (<14hr and >20hr) for the east-west current at 16.6m depth. During the stratified period, the near-inertial Poincare wave is very energetic in 5-10 day bursts (Choi et al., 2012), which is induced by strong wind episodes. Near-inertial energy is seen to dominate energy at this location for much of the stratified period. The dashed box highlighting the elevated wave activities from DOY 200 to 300 will be discussed below.
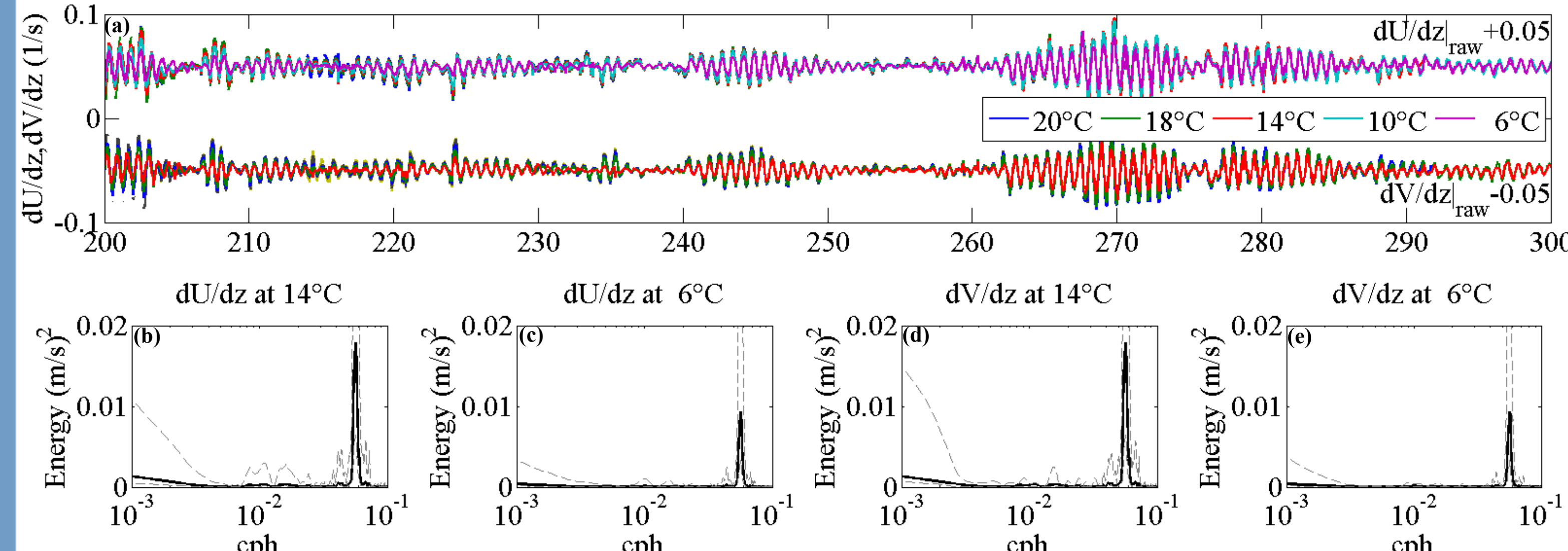


**Fig. 6. Seasonal variations of velocity shear.** (a) The isotherm velocity shear distributions for the east-west (top, shift 0.05s⁻¹ upward) and north-south currents (bottom, shift 0.05 s⁻¹ downward); (b) to (c) are the variance – preserving spectra for east-west velocity shear at the isotherms of 14 and 6°C; (d) to (e) are the same setup for north-south shear. The spectra analyses, (b) to (e) show conclusively that the waves with the near-inertial period dominate the thermocline shear during the stratification period.
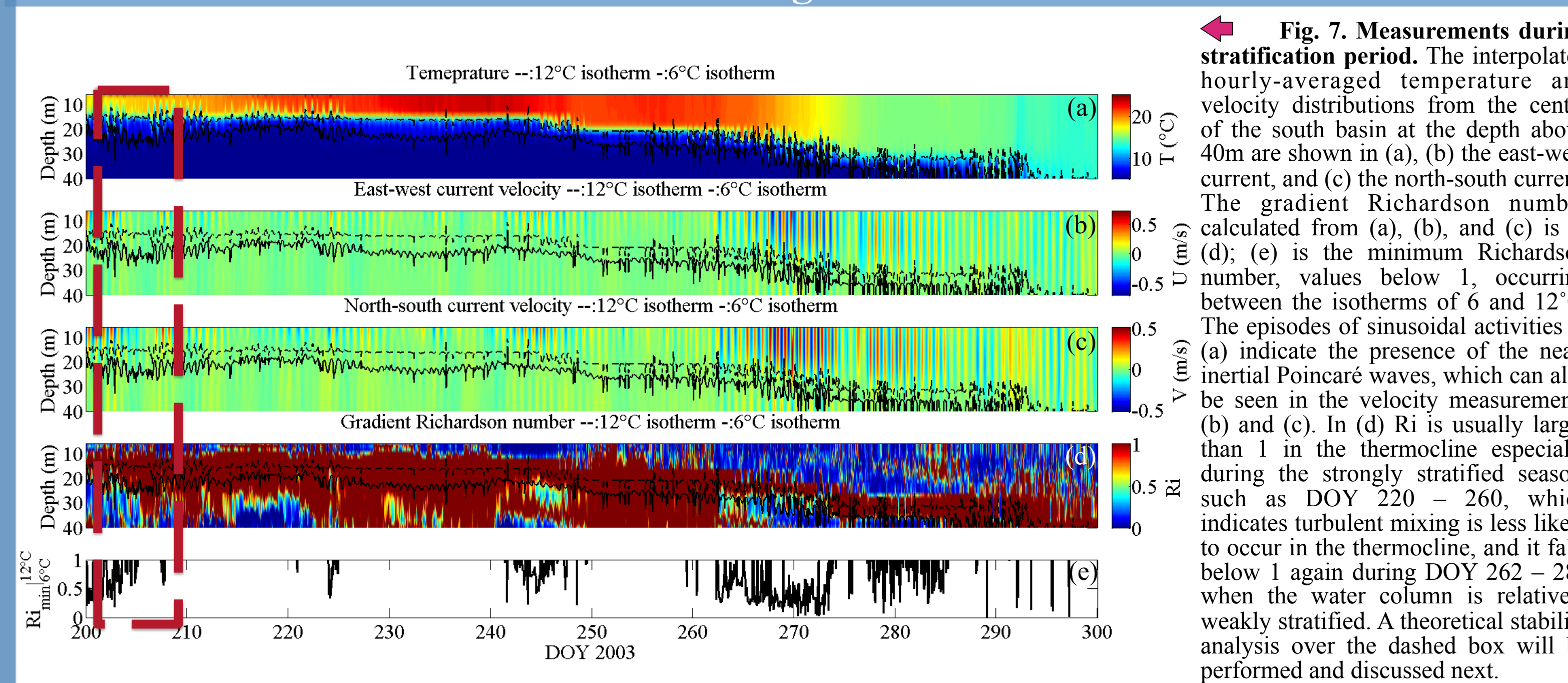
## Measurements during Stratification Period



**Fig. 7. Measurements during stratification period.** The interpolated hourly-averaged temperature and velocity distributions from the center of the south basin at the depth above 40m are shown in (a), (b) the east-west current, and (c) the north-south current. The gradient Richardson number calculated from (a), (b), and (c) is in (d); (e) is the minimum Richardson number, values below 1, occurring between the isotherms of 6 and 12°C. The episodes of sinusoidal activities in (a) indicate the presence of the near-inertial Poincaré waves, which can also be seen in the velocity measurements (b) and (c). In (d) Ri is usually larger than 1 in the thermocline especially during the strongly stratified season, such as DOY 220 – 260, which indicates turbulent mixing is less likely to occur in the thermocline, and it falls below 1 again during DOY 262 – 288 when the water column is relatively weakly stratified. A theoretical stability analysis over the dashed box will be performed and discussed next.
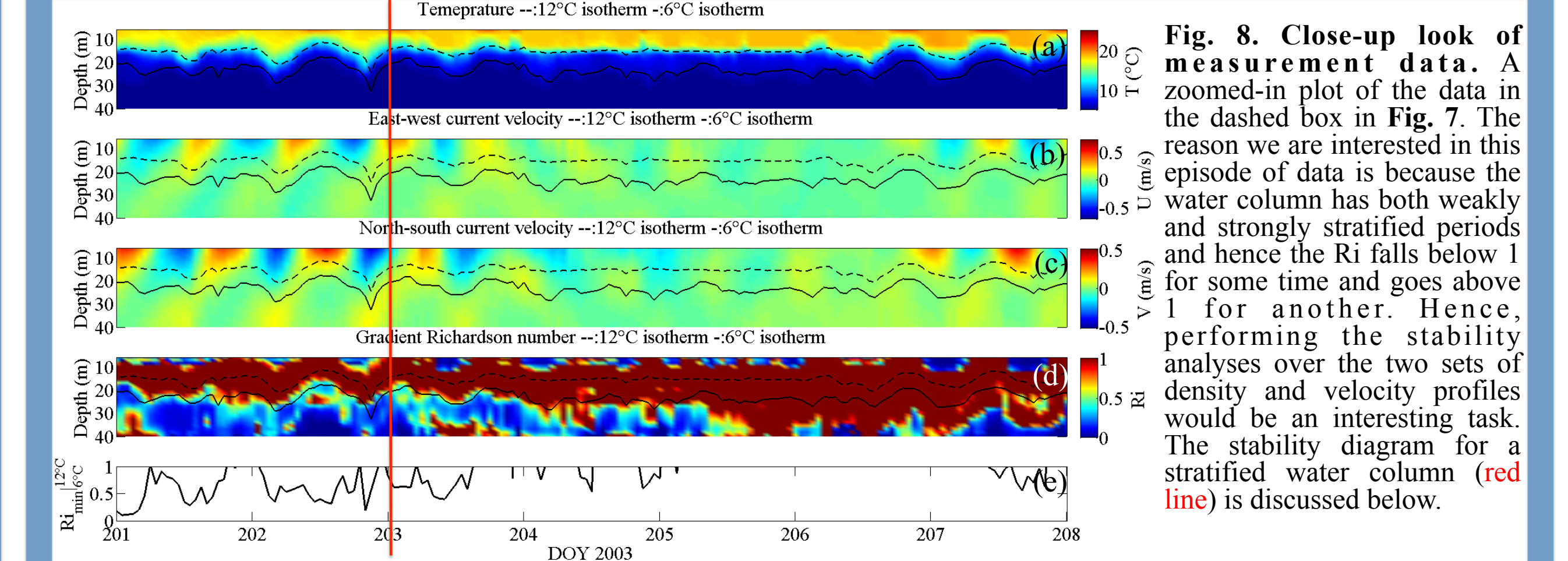


**Fig. 8. Close-up look of measurement data.** A zoomed-in plot of the data in the dashed box in Fig. 7. The reason we are interested in this episode of data is because the water column has both weakly and strongly stratified periods and hence the Ri falls below 1 for some time and goes above 1 for another. Hence, performing the stability analyses over the two sets of density and velocity profiles would be an interesting task. The stability diagram for a stratified water column (red line) is discussed below.
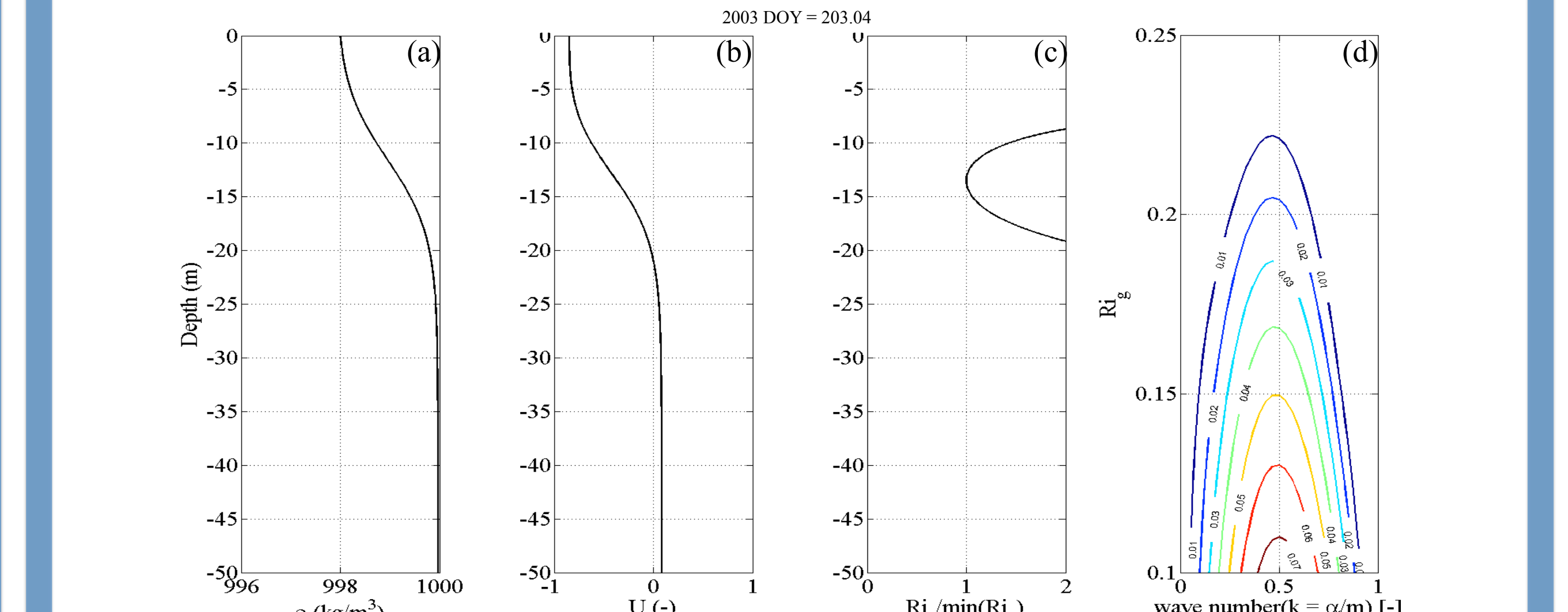
## Stability Analyses



**Fig. 9. Stability diagram for a given set of density and velocity profile.** The temperature profile (a) is chosen on DOY 203.04; (b) is then the velocity from the normal-mode calculation; (c) is the gradient Richardson number based on the given density and velocity profiles; (d) The corresponding stability diagram is obtained from solving the flow fields constructed from (a) and (b) by using a Matlab code, developed by W. Smyth. The result shows that Hazel's (1972) tanh-tanh profiles can be applied to the field measurements.
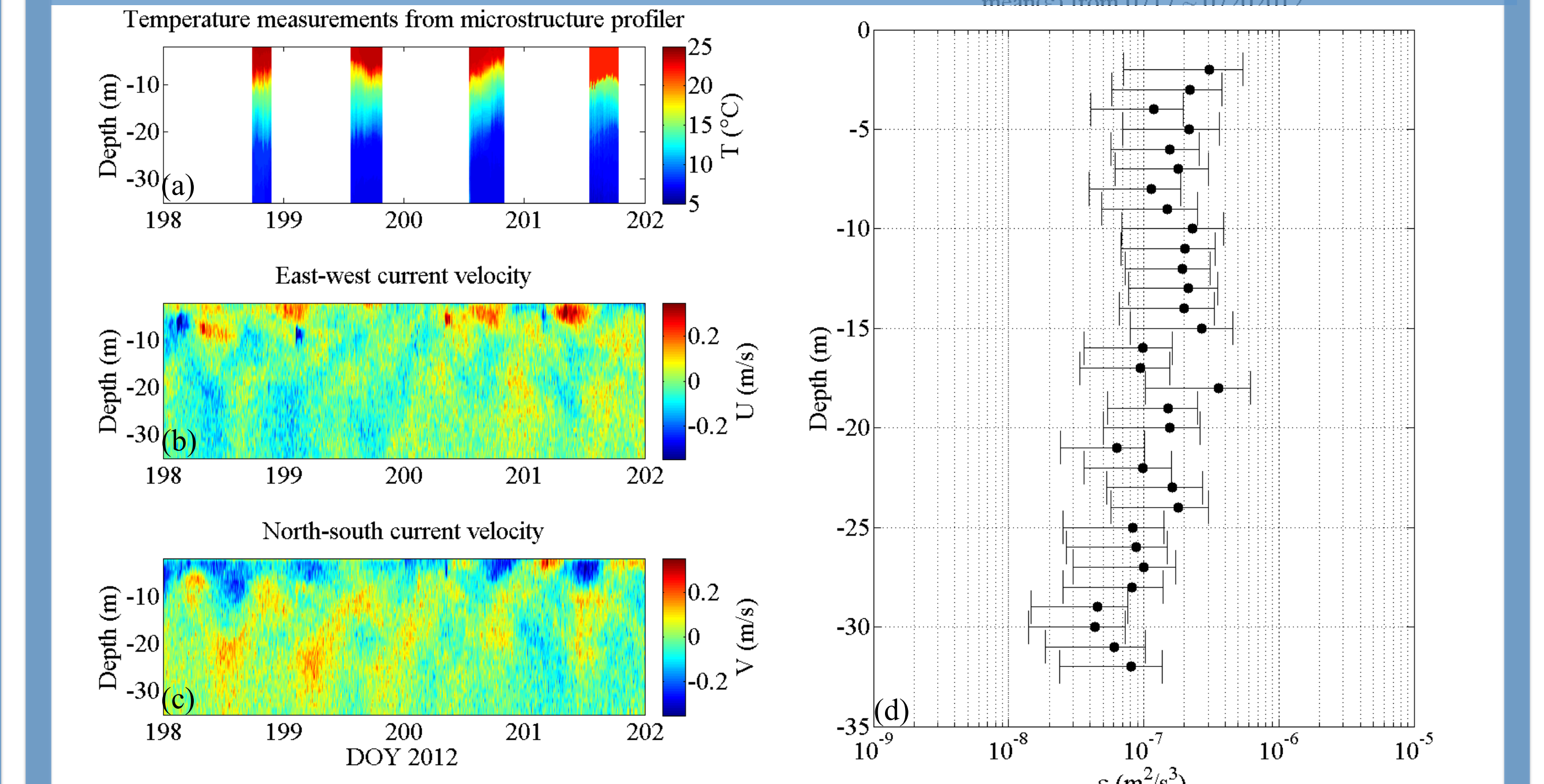
## Future Work



**Fig. 10. Microstructure measurements nearshore.** The temperature measurements from a microstructure profiler (SCAMP) is shown in (a); (b) and (c) are the ADCP current velocity distributions; (d) is the turbulent dissipation rate calculated from the microstructure measurements. The microstructure measurements serve as a direct evidence of turbulent patches. It is used to verify the results from the stability analysis for a given water column. The result from (d) shows that the dissipation rate decays from the free surface to the top of the thermocline (~10m). It then gradually increases with depth in the thermocline (~10-17m). Underneath the thermocline, it shows a decaying trend till the bottom boundary layer (~30m).

## Conclusion and Reference

1. The near-inertial internal Poincaré waves dominate mid-lake currents during the stratification period with a spatially rotating structure and strong thermocline shear.
2. Near-inertial Poincare waves entirely dominate thermocline shear in the lake's interior, suggesting that if instability is occurring, they are the source.
3. Calculated Richardson numbers suggest that wave shear is quite often sufficiently high to generate thermocline instabilities.
4. The stability properties of representative velocity and density profiles do not differ much from canonical results for stratified shear flows. (e.g. Hazel 1972)
5. Microstructure measurements indicates that the thermocline has levels of increased dissipation, particularly at the base of the thermocline. Future work seeks to finalize the correlation between microstructure and shear at this location.

Reference:
1. Choi, J., C. D. Troy, T.-C. Hsieh, N. Hawley, and M. J. McCormick (2012), A year of internal Poincaré waves in southern Lake Michigan, J. Geophys. Res., 117, C07014, doi: 10.1029/2012JC007984.
2. Bouffard, D., Boegman, L.and Yerubandi R. Rao. 2012. Poincaré wave induced mixing in a large lake. Limnol. Oceanogr. 57(4), 1201–1216.
3. Troy, C. D., S. Ahmed, N. Hawley, and A. Goodwell (2012), Cross-shelf thermal variability in southern Lake Michigan during the stratified periods, J. Geophys. Res., 117, C02028, doi: 10.1029/2011JC007148.